

Fig. 7. (continued).

the lower for plane 2, soil. The initial readings for the active pipes (BC, CD and/or DE) and for the fan are also shown. Shaded cells denote the active pipes. The pressure field morphology present in each plane and

setup is readily visualised in the three-dimensional graphics on the right. Plane 1, gravel One particularly prominent finding is the uniformity of pressures on

the gravel plane, irrespective of the distance from the active pipe. The plane 1 values were also higher than in the soil except in sensors near the active pipe, as shown in the 3D graphics in Fig. 7b and the pressure graphs in Fig. 8.

Irrespective of the value observed for the active pipe, the variations recorded by the sensors across plane 1 had a standard deviation of 1 Pa, as shown in Table 1 for the three setups with a single activated pipe (1, 2 and 3), by way of illustration.

The pressure uniformity observed in gravel beds, a finding consistent with prior experimental research (Hung et al., 2018b), appears to be a

common characteristic of such substrates, which establish a broad and uniform pressure field in depressurisation systems.

An abrupt pressure drop was observed in the 55 cm between the active pipe and the gravel plane, with a pressure drop of  $-468.2$  (Pa/m) in the best case scenario (S3: pipe DE). Such pressure drops are routinely found in the first section of soil in depressurisation systems and are steeper in the presence of low permeability. Their intensity declines logarithmically in sections of soil at a farther distance (Gadgil et al., 1991; Health Canada, 2010). In the initial lengths the effect is reinforced by the greater pressure drop associated with the turbulence induced by

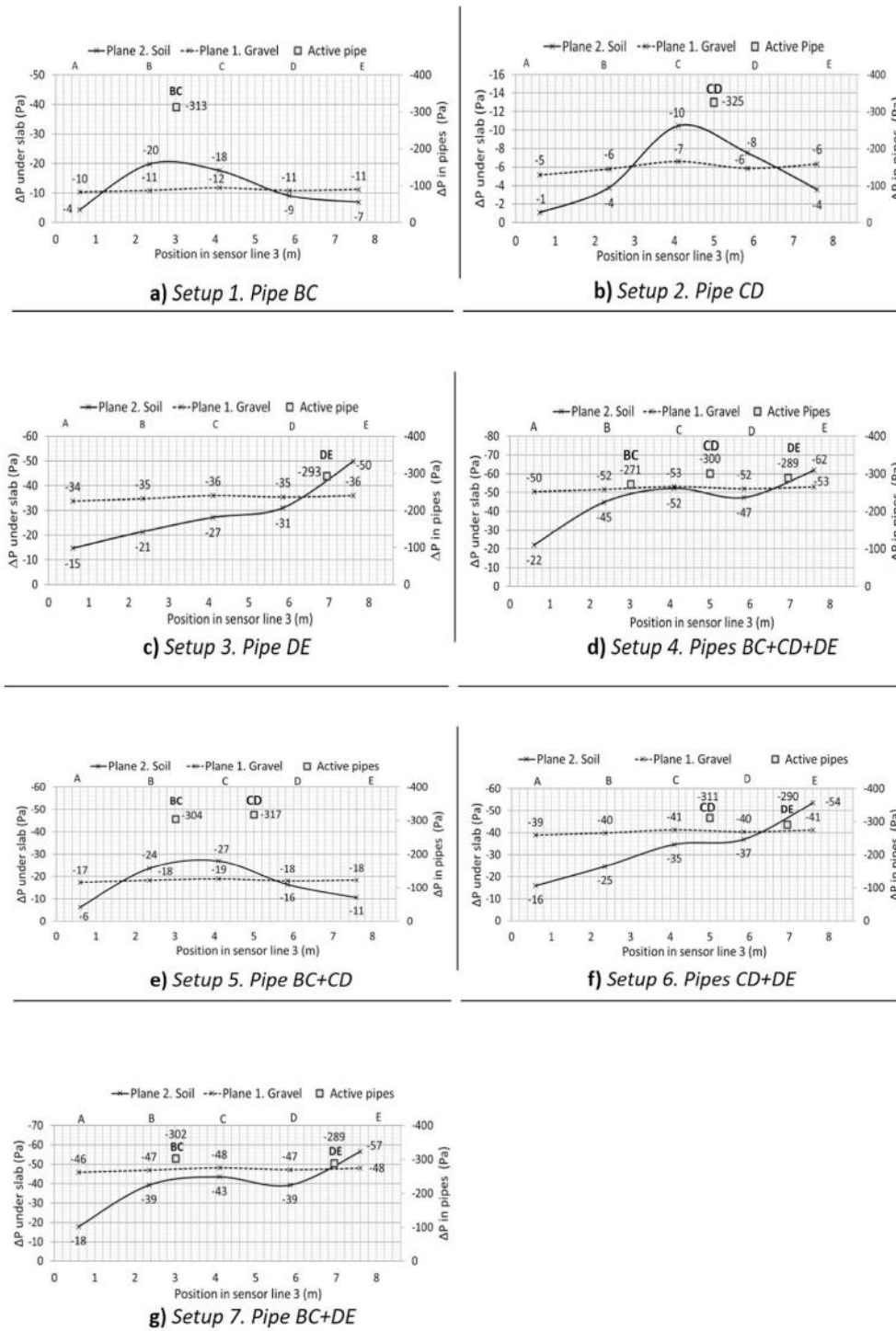


Fig. 8. Differential sub-slab pressure for setups 1 through 7 at a cross-section through sensor line 3 and pipes pressure.

**Table 1**

Extracted air flow rate and pressure in active pipe, mean pressure in gravel and standard deviation, and pressure drop in 55 cm between active pipe and gravel plane.

Test setup	Extract flow in pipe	Pressure in pipe	Mean pressure in plane 1, gravel		Pressure drop $\Delta P/\Delta L$
	(m <sup>3</sup> /h)	(Pa)	(Pa)	SD	(Pa/m)
S1: pipe BC	33.7	-313	-11	1	-549.1
S2: pipe CD	18.9	-325	-6	1	-580.0
S3: pipe DE	53.1	-293	-35	1	-469.1

greater air speed. That development was studied by factoring the Forchheimer equation into Darcy's law (Fuente et al., 2019a):

$$\frac{\Delta P}{\Delta l} = -\frac{\mu}{K_{DF}}v - c\frac{\mu}{K_{DF}}v^2 \quad [1]$$

where  $K_{DF}$  (m<sup>2</sup>) is Darcy-Forchheimer specific permeability and  $c$  (s/m) a constant known as the Forchheimer factor.

Significant differences in the pressure transferred to the gravel by each pipe were also observed: BC (-11 Pa); CD (-6 Pa); DE (-35 Pa). Studying variations in the behaviour of depressurisation systems with the position of the suction point, earlier authors (Frutos and Muñoz, 2018) observed a broader area to be more intensely impacted when that point was located on the perimeter, at a corner or one side, providing it was inside the slab and outward propagation was blocked by the foundation walls. In this study, pipe DE was closest to the perimeter and pipes BC and CD in inner-more positions which might partially explain the higher transfer from the former. Given the scale of the differences, however, the non-uniformity of the soil is believed to have possibly contributed to such a wide variability. As noted in section 3.1, the soil profiles revealed large gravel clusters that might well generate preferential air flow pathways between some pipes and the gravel layer. The data in Table 1 attest to an obvious relationship between extraction flows and pressure transferred to the gravel plane. Lowest resistance was found for the pipe DE setup, where transfer was highest (-35 Pa), whereas highest resistance was observed for the lowest transfer value (-6 Pa).

#### Plane 2, soil

Whilst the pressure distribution in gravel was very uniform at all points irrespective of the distance from the active pipe, the findings for the soil differed in that respect, with pressure varying with distance. The graphs in Fig. 8 plot the pressure on both planes at a cross-section through sensor line 3 (center of the slab) for the seven test setups. Pipe pressure is also shown.

The rise in pressure readings closest to the active pipe was greater in the soil than in the gravel sensors, whilst pressure drop was in keeping with the distance from the pipe/s involved in each setup (3D graphics in Fig. 7b and pressure plots in Fig. 8).

Although pressure varied with distance, pressure drop did not follow a uniform pattern. The data suggested that the gravel layer above may have provided an alternative pathway for pressure propagation and that the pressure detected by the soil sensors distant from the active pipe was the sum of the direct pathway and the pathway through the gravel. As noted, the latter distributed pressure evenly across the entire surface. An example of that hypothesis is shown in the diagram in Fig. 9 for pipe DE, with the pathway to the farthest soil sensor, A'.

An analysis of the two possible pathways provides an explanation for the pressure values observed in distant sensors, which were substantially higher than expected if only the direct pathway were followed.

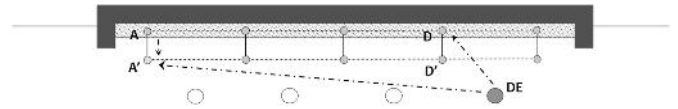


**Fig. 9.** Possible air flow pathways from DE to A': direct, DE-A'; through gravel layer, DE-D-A-A'.

### 3.2. Pressure distribution and pressure drop in the pipe/header pipe system

As the pressure patterns in the pipe system itself, including both above and underground components, were deemed to be of possible interest, the pressures in the aerial header (the most upstream of the components) were compared to the values in each perforated pipe in all the setups studied. As the data in Table 2 show, the pressure in the various setups, with values of 88%–98%, were not significantly lower than in the header. All the pipes might therefore be regarded to receive around 95% of the header pressure, with no major differences observed in that regard between opening only one or any combination of pipes. That finding is promising, inasmuch as it means that a single fan would deliver sufficient pressure for a multi-pipe system with no significant pressure drop in any of the legs.

A comparison of the readings at the head and tail ends of pipe AB (the only one fitted with a tail sensor) yielded the following data:

Head end of AB: -289.7 Pa; tail end of AB: -154.6 Pa; 53% pressure drop.

Air flow entering the pipe along its entire length would contribute to the pressure drop in such perforated elements. That observation might be of interest for perforated system design and calculation of the possible loss of efficacy with distance.

In connection with the latter concern, Fig. 10 shows the pressure readings in the soil and gravel planes in longitudinal sections parallel to the active pipes, revealing pipe behaviour across its length from the header. The figure gives the initial pressure in the pipe and the value expected in each leg assuming the 53% pressure drop to be linearly distributed. Only the readings for single pipes (setups 1, 2 and 3) delivered by the longitudinal line of sensors to the right of each, i.e., line C for S1, D for S2 and E for S3, are shown.

A certain decline in pressures was observed across the longitudinal section on the soil plane, although a number of points did not fit that pattern. As discussed earlier, soil non-uniformity may have induced preferential pathways between sensors in soil and the pipes.

Pressure was observed to be uniform in the gravel plane, as recorded for the overall distribution (section 3.1), with no distance-related variation in pressure.

### 3.3. Pressures reached by combining active pipes

The pressures reached in the gravel and soil planes when two or more perforated pipes were activated simultaneously were compared to the sum of the pressures delivered by each separately, based on the information drawn from the central line of sensors (3).

As Table 3 shows, the empirical pressure readings were practically the same as the sum of the pressures in each pipe, with a margin of error of  $\pm 5\%$  in most cases.

In this size slab and type of gravel layer, moreover, spacing between active pipes was not a significant parameter. The pressure transferred to the gravel plane when two pipes were activated depended not on the spacing (2 m, 4 m or 6 m), but on the pressure contributed by each separately which, as discussed earlier, differed due to the non-uniformity of the substrates between pipe and slab.

The conclusion that might be drawn is that the pressures observed constitute a very close match to those found by summing the effect of each the pipes at issue, irrespective of the distance between them.

The observation to the effect that activation of a larger number of

**Table 2**  
Distribution of pressure across the pipe system for different test setups.

	Pipe pressure (Pa) and % of total in header						Pipe pressure (Pa) by combination and % of total in header							
	BC		CD		DE		BC + CD + DE		BC + CD		CD + DE		BC + DE	
	(Pa)	%	(Pa)	%	(Pa)	%	(Pa)	%	(Pa)	%	(Pa)	%	(Pa)	%
Header	-327	100	-332	100	-320	100	-307	100	-321	100	-316	100	-311	100
BC	-313	96					-271	88	-304	95			-302	97
CD			-325	98			-300	98	-317	99	-311	98		
DE					-293	92	-289	94			-290	91	-289	93

Pressure drop across the 8 m of perforated pipe.

**Table 3**  
Pressure along sensor line 3 in gravel (plane 1) and soil (plane 2), by test setup.

Sensor Line 3		Individual pipes			Combinations			BC + CD			CD + DE			BC + DE			
		BC	CD	DE	BC + CD + DE			Sum	Real	R/S	Sum	Real	R/S	Sum	Real	R/S	
		(Pa)	(Pa)	(Pa)	(Pa)	(Pa)	(Pa)	(Pa)	(Pa)	(Pa)	(Pa)	(Pa)	(Pa)	(Pa)	(Pa)	(Pa)	(Pa)
Plane 1. Gravel	A	-10	-5	-34	-49	-50	102	-15	-17	113	-39	-39	100	-44	-46	105	
	B	-11	-6	-35	-52	-52	100	-17	-18	106	-41	-40	98	-46	-47	102	
	C	-12	-7	-36	-55	-53	96	-19	-19	100	-43	-41	95	-48	-48	100	
	D	-11	-6	-35	-52	-52	100	-17	-18	106	-41	-40	98	-46	-47	102	
	E	-11	-6	-36	-53	-53	100	-17	-18	106	-42	-41	98	-47	-48	102	
Plane 2. Soil	A	-4	-1	-15	-20	-22	110	-5	-6	120	-16	-16	100	-19	-18	95	
	B	-20	-4	-21	-45	-45	100	-24	-24	100	-25	-25	100	-41	-39	95	
	C	-18	-10	-27	-55	-52	95	-28	-27	96	-37	-35	95	-45	-43	96	
	D	-9	-8	-31	-48	-47	98	-17	-16	94	-39	-37	95	-40	-39	98	
	E	-7	-4	-50	-61	-62	102	-11	-11	100	-54	-54	100	-57	-57	100	

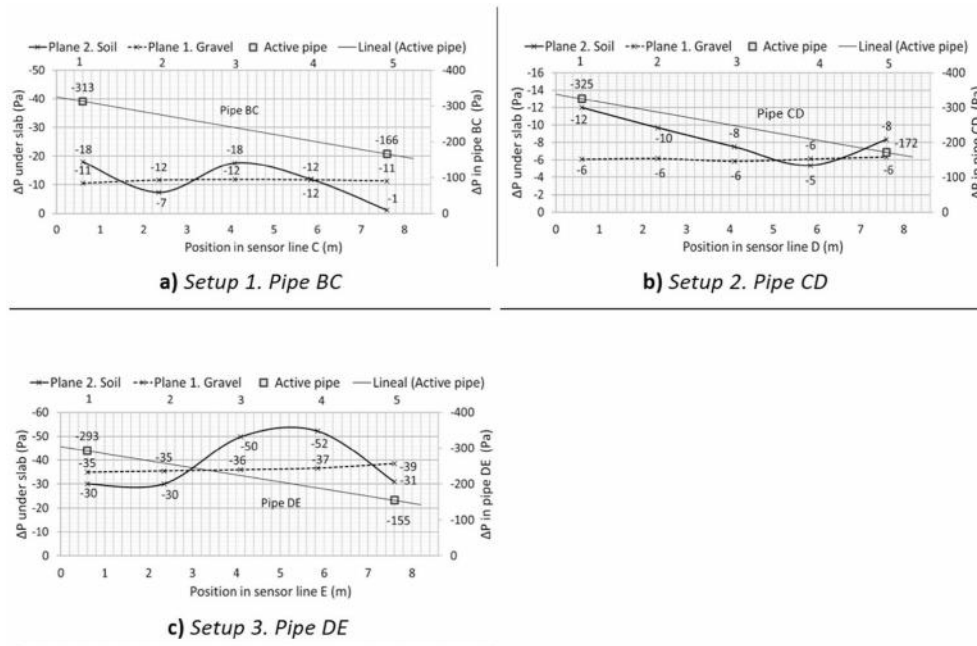


**Fig. 10.** Pressure graphs: a) longitudinal section along sensor line C for setup 1, b) line d for setup 2 and c) line e for setup 3.

pipes entailed higher overall transfer to the gravel plane with no need to raise fan pressure also merits mention in this regard.

**3.4. Relationship between fan power and pressure induced in plane 1, gravel**

A potentiometer was fitted to the fan to study the pressure distribution at the lower power values normally used in depressurisation mitigation solutions.

The variation in the pressure fields beneath the slab (plane 1, gravel) was then measured under three combinations of active pipes at three potentiometer settings: 10 (the maximum), 7 and 5. The correlation between readings in the fan and in gravel is plotted in Fig. 11.

At a given fan setting, higher pressures were recorded in the soil as the number of pipes activated rose, corroborating the earlier observation to that effect (S4>S6>S3).

The data were used to study the relationship between the reduction in fan pressure and its impact on gravel plane pressure. The slope on the

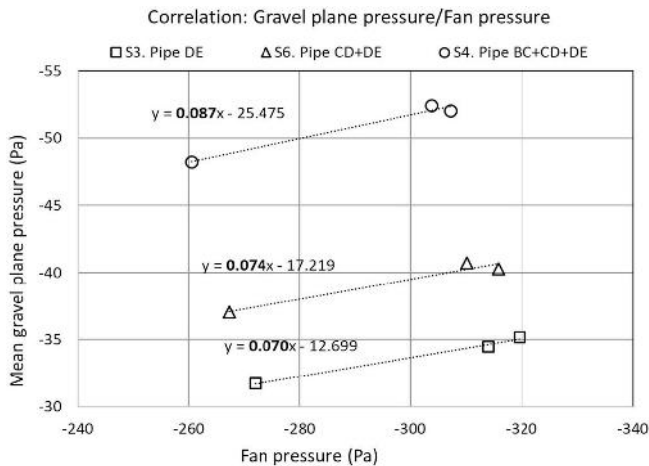


Fig. 11. Gravel plane vs fan pressure in setups 3, 6 and 4.

$(\Delta P_{\text{GRAVEL}}/\Delta P_{\text{FAN}})$  curve was observed to rise when more pipes were active, from 7.0% for pipe DE alone to 8.7% for pipe combination BC + CD + DE. That finding would appear to mean that pressure transfer to the gravel at lower fan power declined more steeply when more pipes were active.

Nonetheless, due to the narrow difference between the settings analysis was not wholly satisfactory. In future studies this effect will be verified with a more sensitive potentiometer.

#### 4. Conclusions

Although depressurisation techniques are deemed to be highly effective, their efficacy depends on a thorough understanding of the fluid physics governing sub-slab pressure fields. Those fields were measured and characterised in this study of the depressurisation generated by a series of parallel perforated pipes underneath a large-scale slab resting on a layer of gravel. Pressure was assessed when each pipe was depressurised separately or in combination with others and at different initial pressures, controlled by a potentiometer. The conclusions drawn from the findings are set out below.

The presence of sub-slab gravel with a permeability of  $10^{-8} \text{ m}^2$  generated a uniform pressure field across the entire  $64 \text{ m}^2$  slab studied. That behaviour was not observed in the natural soil on plane 2, where permeability was  $10^{-12} \text{ m}^2$  and where pressure declined with the distance from the active pipe.

This study therefore reconfirmed the benefits of gravel beds, which extend and raise the depressurisation in SD systems.

Another finding of interest was that the pressure transferred to the gravel plane varied from pipe to pipe. An analysis of the resistance in the soil between each pipe and the gravel plane revealed substantial differences that might be associated with soil non-uniformity, although pipe position relative to slab geometry might also have contributed to that result. The higher values in the outer pipes, also reported in other studies, would be due to their proximity to the foundations, which obstructed pressure field expansion on one side.

The pressure inside any given pipe did not vary when activated separately or in combination with others. At the same time, activating more pipes was found to raise sub-slab depressurisation with no need to raise the fan power. More specifically, the resulting pressure was observed to be nearly identical to the sum of the pressures of each pipe operating separately. In the slab-gravel layer arrangement studied here, that sum of pressure values was shown to depend not on inter-pipe spacing, but rather on the pressure contributed by each pipe separately. That finding may be relevant to the design of multi-pipe systems attached to a single fan, for the inference is that increasing the number of suction points or pipes is more effective than raising extraction power.

This study affords material for characterising perforated pipe-based depressurisation systems. Nonetheless, some of the matters addressed call for further research to confirm patterns and explore new areas, such as the effects of inner foundation lines on pressure propagation or performance in the absence of a gravel bed.

#### Declaration of competing interest

The authors declare that they have no known competing financial interests or personal relationships that could have appeared to influence the work reported in this paper.

#### Acknowledgements

This research was funded by the Spanish National Research Council (CSIC) [RTC-2015-3464-5], an entity under the aegis of the country's Ministry of Economy and Competitiveness. The study was conducted at the Eduardo Torroja Institute for Construction Science (IETcc), Spain, in conjunction with the University of Cantabria and Geocisa, S.A.

#### References

- ASTM International, U.S., 2013. ASTM-D6539. Standard Test Method for Measurement of the Permeability of Unsaturated Porous Materials by Flowing Air.
- KASPAR, J., Prokop, P., Matolín, M., 1993. FH-1, equipment for in situ permeability measurements, in Radon investigation in CS. Czech Geol. Surv. Spec. Pap. 4, 4–8.
- Abdelouhab, M., Collignan, B., Allard, F., 2010. Experimental study on passive Soil Depressurisation System to prevent soil gaseous pollutants into building. Build. Environ. 45, 2400–2406. <https://doi.org/10.1016/j.buildenv.2010.05.001>.
- Andersen, C.E., 2001. Numerical modelling of radon-222 entry into houses: an outline of techniques and results. Sci. Total Environ. 272, 33–42. [https://doi.org/10.1016/S0048-9697\(01\)00662-3](https://doi.org/10.1016/S0048-9697(01)00662-3).
- Bonnefous, Y.C., Gadgil, A.J., Fisk, W.J., Prill, R.J., 1992. Field study and numerical simulation of sub slab ventilation systems. Environ. Sci. Technol. 26, 1752–1759.
- Collignan, B., Kelly, P.O., Pilch, E., 2004. Basement depressurisation using dwelling mechanical exhaust ventilation system. In: 4th European Conference on Protection against Radon at Home and at Work. Praha, Czech Republic.
- Collignan, B., Lorkowski, C., Améon, R., 2012. Development of a Methodology to Characterize Radon Entry in Dwellings, vol. 57, pp. 176–183. <https://doi.org/10.1016/j.buildenv.2012.05.002>.
- Cosma, C., Papp, B., Cucos Dinu, A., Sainz, C., 2015. Testing radon mitigation techniques in a pilot house from Băița-Ștei radon prone area (Romania). J. Environ. Radioact. 140, 141–147. <https://doi.org/10.1016/j.jenvrad.2014.11.007>.
- Ministerio de Fomento, 2006. In: REAL DECRETO 314/2006, de 17 de marzo, por el que se aprueba el Código Técnico de la Edificación, REAL DECRETO 314/2006, de 17 de marzo, por el que se aprueba el Código Técnico de la Edificación. <https://www.boe.es/boe/dias/2006/03/28/pdfs/A11816-11831.pdf>.
- Diallo, T.M.O., Collignan, B., Allard, F., 2015. Air flow models for sub-slab depressurization systems design. Build. Environ. 87, 327–341. <https://doi.org/10.1016/j.buildenv.2015.01.017>.
- Diallo, T.M.O., Collignan, B., Allard, F., 2018. Analytical quantification of the impact of sub-slab gravel layer on the airflow from soil into building substructures. Build. Simul. 11, 155–163. <https://doi.org/10.1007/s12273-017-0375-y>.
- EPA Environmental Protection Agency, 1994. Making the Multilateral System More Effective. A TECHNICAL GUIDANCE MANUAL.
- Font, L., Baixeras, C., 2003. The RAGENA dynamic model of radon generation, entry and accumulation indoors. Sci. Total Environ. 307, 55–69.
- Fowler, C., Williamson, A., Pyle, B., Belzer, F., Coker, R., 1991. Handbook: sub-slab depressurization for low permeability fill material design and installation of a home radon reduction system. EPA/625/6-91/029, 1991.
- Friedmann, H., Baumgartner, A., Bernreiter, M., Gräser, J., Gruber, V., Kabrt, F., Kaineder, H., Maringer, F.J., Ringer, W., Seidel, C., Wurm, G., 2017. Indoor radon, geogenic radon surrogates and geology – investigations on their correlation. J. Environ. Radioact. 166, 382–389. <https://doi.org/10.1016/j.jenvrad.2016.04.028>.
- Frutos, B., Muñoz, E., 2018. Field pressure studies for understanding depressurization techniques. In: Radon Outcomes on Mitigation Solutions (ROOMS). Lugano.
- Frutos, B., Olaya, M., Esteban, J.L., 2011. Extraction systems as construction techniques to prevent radon entry in homes. Inf. La Constr. 63, 22–36. <https://doi.org/10.3989/ic.09.056>.
- Frutos Vazquez, B., Olaya Adan, M., Quindos Poncela, L.S., Sainz Fernandez, C., Fuente Merino, I., 2011. Experimental study of effectiveness of four radon mitigation solutions, based on underground depressurization, tested in prototype housing built in a high radon area in Spain. J. Environ. Radioact. <https://doi.org/10.1016/j.jenvrad.2011.02.006>.
- Fuente, M., Muñoz, E., Sicilia, I., Goggins, J., Hung, L.C., Frutos, B., Foley, M., 2019a. Investigation of gas flow through soils and granular fill materials for the optimisation of radon soil depressurisation systems. J. Environ. Radioact. <https://doi.org/10.1016/j.jenvrad.2018.12.024>.

- Fuente, M., Rábago, D., Goggins, J., Fuente, I., Sainz, C., Foley, M., 2019b. Radon mitigation by soil depressurisation case study: radon concentration and pressure field extension monitoring in a pilot house in Spain. *Sci. Total Environ.* 695, 133746. <https://doi.org/10.1016/j.scitotenv.2019.133746>.
- Gadgil, A.J., Bonnefous, Y.C., Fisk, W.J., Prill, R.J., Nematollahi, A., 1991. Influence of Subslab Aggregate Permeability on SSV Performance, Environmental Science and Technology. Lawrence Berkeley Laboratory. LBL-31160.
- Garbesi, K., Robinson, A.L., Sextro, R.G., Nazaroff, W.W., 1999. Radon entry into houses. *Health Phys.* 77, 183–191. <https://doi.org/10.1097/00004032-199908000-00008>.
- Gaskin, J., Coyle, D., Whyte, J., Krewski, D., 2018. Global estimate of lung cancer mortality attributable to residential radon. *Environ. Health Perspect.* 126, 057009 <https://doi.org/10.1289/EHP2503>.
- Groves-Kirkby, C.J., Crockett, R.G.M., Denman, A.R., Phillips, P.S., 2015. A critical analysis of climatic influences on indoor radon concentrations: implications for seasonal correction. *J. Environ. Radioact.* 148, 16–26. <https://doi.org/10.1016/j.jenvrad.2015.05.027>.
- Health Canada, 2010. Reducing Radon Levels in Existing Homes. A Canadian Guide for Professional Contractors.
- Hintenlang, D.E.A.-A., 1992. Pressure differentials for radon entry coupled to periodic atmospheric pressure variations. *Indoor Air* 208–215, 1992.
- Hung, L.C., Goggins, J., Fuente, M., Foley, M., 2018a. Characterisation of specified granular fill materials for radon mitigation by soil depressurisation systems. *Construct. Build. Mater.* 176, 213–227. <https://doi.org/10.1016/j.conbuildmat.2018.04.210>.
- Hung, L.C., Goggins, J., Fuente, M., Foley, M., 2018b. Investigation of sub-slab pressure field extension in specified granular fill materials incorporating a sump-based soil depressurisation system for radon mitigation. *Sci. Total Environ.* 637, 1081–1097. <https://doi.org/10.1016/J.SCITOTENV.2018.04.401>, 638.
- Hung, L.C., Goggins, J., Croxford, C., Foley, M., 2019. Large-scale experimental investigations of specified granular fill materials for radon mitigation by active and passive soil depressurisations. *J. Environ. Radioact.* 207, 27–36. <https://doi.org/10.1016/J.JENVRAD.2019.05.018>.
- IARC, 1998. On the Evaluation of the Carcinogenic Risk to Humans. IARC MONOGRAPHS.
- Jiránek, M., Neznal, M., Neznal, M., 2008. Mitigation of ineffective measures against radon. *Radiat. Protect. Dosim.* 130, 68–71. <https://doi.org/10.1093/rpd/ncn120>.
- Muñoz, E., Frutos, B., Olaya, M., Sánchez, J., 2017. A finite element model development for simulation of the impact of slab thickness, joints, and membranes on indoor radon concentration. *J. Environ. Radioact.* 177, 280–289. <https://doi.org/10.1016/j.jenvrad.2017.07.006>.
- Nazaroff, W.W., 1988. Predicting the rate of <sup>222</sup>Rn entry from soil into the basement of a dwelling due to pressure-driven air flow. *Radiat. Protect. Dosim.* 24, 199–202. <https://doi.org/10.1093/oxfordjournals.rpd.a080269>.
- Nazaroff, W.W., Moed, B.A., Sextro, R.G., Nero Jr., A.V., 1988. Soil as a source of indoor radon, generation, migration, and entry. In: *Radon and its Decay Products in Indoor W.W. Nazaroff*, pp. 57–112. New York.
- Neznal, Matej, Neznal, Martin, 2005. Permeability as an important parameter for radon risk classification of foundation soils. *Ann. Geophys.* 48, 175–180. <https://doi.org/10.4401/ag-3192>.
- Neznal, Matej, Neznal, Martin, Matolín, M., Barnet, I., Mikšová, J., 2004. New method for assessing the radon risk of building sites. *Czech Geol. Surv. Spec. Pap.*
- Reddy, T.A., Gadsby, K.J., Black, H.E., Harrje, D.T., Sextro, R.G., 1991. Modeling air flow dynamics in radon mitigation systems: a simplified approach. *J. Air Waste Manag. Assoc.* 41, 1476–1482. <https://doi.org/10.1080/10473289.1991.10466946>.
- Robinson, A.L., 1996. Radon Entry into Buildings : Effects of Atmospheric Pressure Fluctuations and Building Structural Factors. Thesis.
- Roserens, G.-A., Johner, H.-U., Piller, G., Imbaumgarten, P., 2000. Swiss Radon Handbook. Swiss Federal Office of Public Health, Bern.
- Ruano-Ravina, A., Figueiras, A., Barros-Dios, J.M., 2003. Lung cancer and related risk factors: an update of the literature. *Publ. Health* 117, 149–156. [https://doi.org/10.1016/S0033-3506\(02\)00023-9](https://doi.org/10.1016/S0033-3506(02)00023-9).
- Scivyer, C., 2013. RADON SOLUTIONS IN HOMES Radon sump systems, GOOD REPAIR GUIDE. *GRG* 37, 3.
- Sicilia, I., Aparicio, S., Frutos, B., Muñoz, E., González, M., Anaya, J.J., 2019. A multisensor system for the characterization of the field pressure in terrain. Accuracy, response, and adjustments. *Sensors* 19, 3942. <https://doi.org/10.3390/s19183942>.
- Vasilyev, A.V., Zhukovsky, M.V., 2013. Determination of mechanisms and parameters which affect radon entry into a room. *J. Environ. Radioact.* 124, 185–190. <https://doi.org/10.1016/j.jenvrad.2013.04.014>.
- WHO, 2009. Who Handbook on Indoor Radon - A Public Health Perspective, vol. 110. World Heal. <https://doi.org/10.1080/00207230903556771>. Organ.
- Yang, J., Busen, H., Scherb, H., Hürkamp, K., Guo, Q., Tschiersch, J., 2019. Modeling of radon exhalation from soil influenced by environmental parameters. *Sci. Total Environ.* 656, 1304–1311. <https://doi.org/10.1016/J.SCITOTENV.2018.11.464>.
- Zafirir, H., Barbosa, S.M., Malik, U., 2013. Differentiation between the effect of temperature and pressure on radon within the subsurface geological media. *Radiat. Meas.* 49, 39–56. <https://doi.org/10.1016/J.RADMEAS.2012.11.019>.